James P. Verdin
Bureau of Reclamation
Denver, CO 80225

Monitoring Water Quality Conditions in a Large Western Reservoir with Landsat Imagery

Correction of Landsat data for sun angle and atmospheric effects permitted estimation of reservoir conditions for dates without surface sampling data.

Abstract: *Seven Landsat multispectral scanner scenes were processed to portray water quality conditions in Flaming Gorge Reservoir, a large Bureau of Reclamation impoundment in Utah and Wyoming. Concurrent surface sampling data were available for four of the seven scenes. A deterministic approach employing an atmospheric radiative transfer model was used to account for effects of sun angle and atmosphere in the Landsat imagery. This permitted the development of water quality predictive regression equations using surface sampling data from all four dates at once. It also permitted the estimation of reservoir conditions for the three scenes for which no concurrent surface sampling was carried out. The two equations, providing estimates of Secchi transparency and chlorophyll a concentration, were used to monitor the year-to-year spatial variation of trophic zones in the reservoir.*

Introduction

Many investigators have successfully used Landsat multispectral scanner digital imagery in lake and reservoir water quality studies. Recent examples include the work of Martin *et al.* (1983) and Lillesand *et al.* (1983). They used Landsat and surface sampling data to perform trophic classifications of large numbers of lakes in Wisconsin and Minnesota, respectively. Meinert *et al.* (1980) and Grimshaw *et al.* (1980) performed similar studies of large reservoirs. A useful review of the literature describing the application of remote sensing to surface water quality studies is provided by Witzig and Whitehurst (1981).

The Bureau of Reclamation is responsible for the management of over 300 reservoirs throughout the 17 Western States. Many of these reservoirs are of large areal extent in remote locations and, consequently, the monitoring of their water quality conditions poses a considerable challenge. Surface sampling designs must be extensive enough to sample all zones of limnological significance while staying within constraints imposed by the limited availability of funds, personnel, and equipment. This paper reports on recent work by the Bureau to investigate the incorporation of remote sensing in reservoir water quality sampling design in order to increase the benefits derived from sampling efforts.

Most remote sensing water quality studies make use of digital imagery and concurrently acquired surface sampling measurements. Correlations between measurements at sample sites and scanner data at these same points are exploited to develop predictive equations for water quality parameters or trophic state indexes. The equations are then used to characterize conditions for all surface water appearing in the scene. A unique set of equations is developed for each scene. Initial efforts of the Bureau of Reclamation were of this type (Verdin and Wegner, 1983). It became apparent that Landsat imagery could be of even greater utility if the sun angle and atmospheric effects in the data could be removed. This would permit the development of a single set of water quality predictive regression equations from concurrent surface and satellite observations collected on multiple dates. It would also permit the application of the resulting predictive

Photogrammetric Engineering and Remote Sensing,
Vol. 51, No. 3, March 1985, pp. 343-353.

0099-1112/85/5103-0343$02.25/0

equations to the estimation of reservoir water quality conditions with imagery obtained on dates when there were no surface sampling crews in the field.

Description of Study Area

Flaming Gorge Reservoir is a large impoundment at an elevation of 2000 metres on the Green River, a major tributary of the Upper Colorado River Basin. The dam, located in northeastern Utah, was completed in 1963. The reservoir extends 125 kilometres upstream of the damsite, well into southwestern Wyoming. Annual filling of the reservoir is achieved primarily by spring snowmelt from the Uinta, Wind River, and Wyoming ranges of the Rocky Mountains. The stored waters are used to produce hydroelectric power and to meet downstream water supply commitments through the year. The reservoir and adjacent lands comprise the Flaming Gorge National Recreation Area.

Wegner (1982) has documented and analyzed seasonal changes in the spatial distribution of chlorophyll *a* concentrations and Secchi disk transparency since the reservoir was first filled. His analyses showed that Flaming Gorge Reservoir can be divided into three hydrodynamic water quality zones: the riverine inflow area, a transition zone, and the lacustrine main body of the reservoir. These zones are indicated in Figure 1. The inflow area is characterized by high turbidity, extensive mixing, and high nutrient concentrations. The transition zone exhibits reduced sediment turbidity and high primary productivity. The location of the transition zone varies from season to season and annually as a function of reservoir elevation, meteorological conditions, inflow patterns, and hydrodynamics. Waters of the main body are very clear with low levels of primary productivity.

Surface Sampling Data

Limnological sampling surveys typically involve measurement of a variety of water quality parameters, including nutrient concentration, temperature, light penetration, conductivity, dissolved oxygen, heavy metals, chlorophyll concentrations, and samples of plankton and benthos. Only those characteristics which affect the optical properties of reservoir surface waters, either directly or by means of a companion substance, can be expected to correlate with Landsat multispectral scanner data. In this study, use was made of measurements of Secchi transparency and chlorophyll *a* concentration at less than 1 metre depth. These variables are often good indicators of trophic state and had correlated well with remote sensing data in date-specific studies of Flaming Gorge Reservoir (Verdin and Wegner, 1983). Measurements were available for four dates when Landsat imagery of the reservoir had been acquired. The data were gathered by the Environmental Protection Agency, the U.S. Geological Survey, and the Bureau of Reclamation. They are summarized in Table 1.

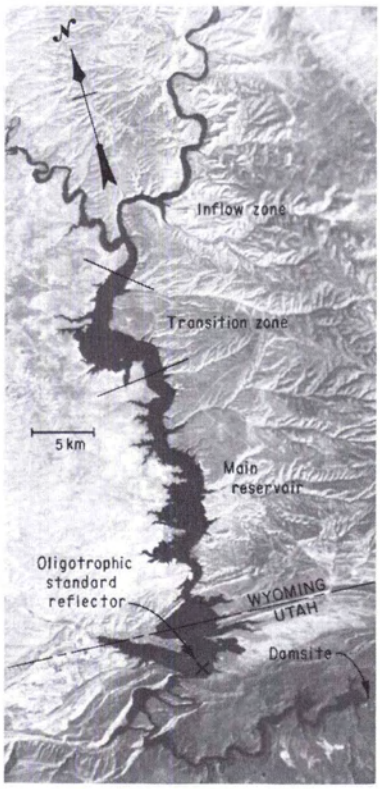

Fig. 1. 24 August 1982 band 7 Landsat scene of Flaming Gorge Reservoir with locations of inflow, transition, and lacustrine zones indicated.

Landsat Data

Computer compatible tapes were obtained for the Landsat scenes of Flaming Gorge Reservoir acquired on 22 September 1975, 2 August 1978, 9 September 1981, and 24 August 1982. As mentioned before, concurrently acquired surface sampling data were available for these dates. In addition, scenes showing the reservoir on 17 September 1976, 18 October 1977, and 13 October 1978, were purchased from the EROS Data Center, Sioux Falls, South Dakota. No surface sampling had been carried out during the 1976 through 1978 algae bloom periods (late August through October), and it was hoped that analysis of these images would fill an informational gap. The choice of dates for these seasons was based on the availability of cloud-free imagery and the judgment of those familiar with the reservoir during the period in question. In all cases, data without geometric correction were purchased, except for the 9 September 1981 scene, when this format could not be provided. The preference for this format is due to the effects along shorelines of the cubic convolution interpolation algorithm,

TABLE 1. SURFACE SAMPLING DATA GATHERED AND CORRESPONDING MEAN LANDSAT DIGITAL COUNTS

Date	Agency	Station	Secchi depth (m)	Chlorophyll *a* (mg/m^3)	Band 4	Band 5	Band 6
22 September 75	EPA	EPA1	0.6	12.3	15.4	12.6	5.7
22 September 75		EPA2	0.6	6.9	15.0	12.0	5.0
22 September 75		EPA3	1.5	16.9	11.3	8.8	6.7
22 September 75		EPA4	4.6	3.3	8.1	5.7	1.7
22 September 75		EPA6	4.6	3.1	8.7	5.4	2.1
22 September 75		EPA7	5.5	2.7	8.2	5.5	1.9
22 September 75		EPA8	4.6	2.7	7.1	4.5	1.8
22 September 75		EPA9	5.0	2.4	6.8	4.3	1.7
24 September 75	USGS	GS1	5.1	—	6.9	4.9	1.9
25 September 75		GS2	6.5	—	6.8	5.1	1.8
25 September 75		GS5	7.0	—	8.7	5.4	2.1
25 September 75		GS6	7.5	—	8.1	5.4	2.1
24 September 75		GS8	6.0	—	8.3	5.4	2.2
23 September 75		GS9	5.5	—	8.2	6.1	2.6
23 September 75		GS10	5.2	—	7.8	5.9	2.1
23 September 75		GS11	4.5	—	8.2	6.4	2.2
22 September 75		GS13	3.1	—	9.9	8.0	4.1
22 September 75		GS14	2.6	—	9.8	7.2	4.2
23 September 75		GS15	3.0	—	9.3	7.4	3.0
23 September 75		GS17	1.5	—	12.5	10.5	4.8
23 September 75		GS20	3.0	—	11.7	9.0	4.8
23 September 75		GS21	1.5	—	12.1	10.2	5.2
23 September 75		GS22	0.9	—	17.8	14.1	8.0
23 September 75		GS23	0.6	—	17.6	14.6	8.8
2 August 78	EPA	1	0.6	8.670	20.6	18.8	7.6
2 August 78		2	0.7	7.412	15.4	12.2	5.3
2 August 78		3	0.7	9.734	20.6	18.1	8.7
2 August 78		4	1.5	4.495	13.4	10.8	5.0
2 August 78		5	1.6	3.567	12.6	9.7	4.8
2 August 78		6	3.7	4.917	10.3	7.6	3.0
2 August 78		7	4.0	2.806	10.3	8.1	3.9
2 August 78		8	3.0	2.148	10.3	8.6	3.8
2 August 78		9	5.0	2.549	9.7	6.4	2.3
2 August 78		10	3.8	4.001	11.3	7.2	3.4
2 August 78		11	6.0	2.361	10.7	7.0	3.3
2 August 78		12	7.1	3.002	10.1	6.2	2.9
2 August 78		13	5.4	2.123	11.6	7.4	3.3
2 August 78		14	3.6	3.463	13.1	7.9	3.6
2 August 78		15	3.3	1.735	13.6	8.6	3.4
2 August 78		16	3.6	1.656	12.2	7.5	3.2
9 September 81	USBR	FG4	8.5	1.72	9.8	6.4	2.8
9 September 81		FG5.1	6.7	0.88	10.9	8.2	3.0
9 September 81		FG10	5.5	1.55	10.4	7.9	3.4
9 September 81		FG10.1	4.9	1.06	10.7	7.6	3.0
9 September 81		FG10.2	4.6	1.21	10.3	7.9	2.8
9 September 81		FG10.3	3.4	3.07	12.3	8.9	3.8
9 September 81		FG12	2.7	5.24	13.3	10.9	5.6
9 September 81		FG15	2.3	6.29	13.7	10.4	5.0
9 September 81		FG15.1	1.7	20.00	15.9	11.3	5.9
9 September 81		FG15.2	1.5	—	18.4	13.6	6.9
9 September 81		FG15.3	1.2	—	21.6	17.0	13.0
9 September 81		FG15.4	1.1	—	23.9	17.0	8.8
9 September 81		FG15.5	0.3	—	30.6	31.7	14.4
9 September 81		FG20	1.8	5.35	15.8	11.7	5.1
9 September 81		FG20.1	1.8	—	15.1	10.9	4.3
9 September 81		FG20.2	1.8	—	17.2	11.2	4.1
9 September 81		FG22	1.7	4.19	17.7	12.9	4.9
9 September 81		FG22.1	0.9	—	26.2	19.3	8.0
9 September 81		FG22.2	0.2	—	36.0	38.0	14.0
9 September 81		FG22.3	0.2	—	35.8	39.1	19.6
24 August 82	USBR	FG2	6.1	1.33	11.1	6.3	2.9
24 August 82		FG4	6.1	0.93	12.0	7.5	3.5
24 August 82		FG5	6.1	1.36	12.4	8.0	3.8
24 August 82		FG10	3.4	4.26	12.7	8.6	4.1
24 August 82		FG12	3.4	25.30	16.7	10.7	8.0
24 August 82		FG15	2.1	19.61	18.0	11.5	9.0
24 August 82		FG15.1	2.1	14.15	17.0	11.5	7.8
24 August 82		FG20	0.9	20.11	18.7	13.0	9.7
24 August 82		FG22	0.9	17.41	21.0	15.0	8.8

which were first noted by Olsen *et al.* (1981) and were further described by Verdin (1983).

Upon receipt of the imagery, it was entered onto an interactive digital image processing system and displayed on a video console. Sampling stations were located by visual inspection while referring to maps supplied with the surface data. In some cases, sample site locations had been marked on U.S. Geological Survey 7.5-minute quadrangle maps and the same spots could be found in the scene quite reliably. In other cases, only small-scale maps and an estimate of distance miles above the dam were available, and site identification was made with less certainty. In part to compensate for this uncertainty, mean brightness counts were recorded for three-by-three pixel blocks at the identified points. Exceptions to this practice were made in the narrow arms of the reservoir, when a three-by-three block would take in shoreline pixels, and also in cases where linearly shaped algal blooms would not fill such a block. Mean digital counts in bands 4, 5, and 6 for the sample sites are presented in Table 1. Sunlight in the band 7 wavelengths penetrates clear water to a depth of only 10 cm (Hoffer, 1978), and for this reason band 7 data were not employed for surface water quality analysis. The spectral identities of the Landsat bands are presented in Table 2.

Atmospheric Correction of Landsat Data

Use of satellite image data from multiple dates requires that sun angle and atmospheric effects be accounted for in order to infer the reflectance of targets on the Earth's surface. Ahern *et al.* (1977) described a technique for doing this which does not require any ground measurement of solar radiation. The method was applied successfully by Richardson *et al.* (1980). For these reasons, the technique was selected for the study of Flaming Gorge Reservoir. In this approach, the simplified model of the interaction of solar radiation with the atmosphere is stated as

$$L_{sat} = r\,T\,H_{tot} + L_p \qquad (1)$$

where L_{sat} is the radiance sensed by Landsat in a given spectral band (mW/cm^2 sr), r is target reflectance, defined as the ratio of upwelling radiance to downwelling irradiance (sr^{-1}), T is atmospheric transmittance from surface to satellite (dimensionless), H_{tot} is total irradiance incident on a horizontal surface at the bottom of the atmosphere (mW/cm^2), and L_p is atmospheric path radiance (mW/cm^2 sr).

Table 2. Spectral Bands of the Landsat Multispectral Scanner

Band*	Wavelength (μm)	Color/spectrum
4	0.50–0.60	Green
5	0.60–0.70	Red
6	0.70–0.80	Near infrared
7	0.80–1.10	Near infrared

* With the launch of Landsat 4, the MSS bands have been renumbered 1 through 4. However, only one scene used in this study was acquired by that satellite, so the old numbering scheme has been retained.

Values of L_{sat} are computed from the digital counts making up a Landsat scene by the following equation (Robinove, 1982):

$$L_{sat} = \frac{DC}{DC_{max}}(L_{max} - L_{min}) + L_{min} \qquad (2)$$

where DC is the digital count for a pixel of interest, DC_{max} is the maximum digital count for the band of consideration (127 for bands 4, 5, and 6; 63 for band 7), L_{max} is the radiance yielding detector saturation, and L_{min} is the lowest radiance measured by the detector. Values of L_{max} and L_{min} for Landsats 1 through 4 are presented in Table 3. Target reflectance, r, is an observational quantity and differs from ρ, the reflectance of a Lambertian surface, according to the relation:

$$\rho = \pi r \qquad (3)$$

where ρ is a dimensionless quantity representing the ratio of upwelling to downwelling irradiance. Atmospheric transmittance, T, from surface to satellite is defined as

$$T = e^{(-\tau \sec \theta_n)} \qquad (4)$$

where τ is the total optical depth of the atmosphere and θ_n is the satellite nadir view angle. Total irradiance, H_{tot}, is made up of direct and diffuse insolation: i.e.,

$$H_{tot} = H_o \cos Z\, e^{(-\tau \sec Z)} + H_{sky}. \qquad (5)$$

In Equation 5, H_o is the solar irradiance at the top of the Earth's atmosphere (mW/cm^2), Z is the solar zenith angle, and H_{sky} is the irradiance on a horizontal surface due to diffuse skylight. Richardson *et al.* (1980) cite several sources for values of H_o, including Thekaekara *et al.* (1969) and Rogers and Peacock (1973). Diffuse sky irradiance, H_{sky}, depends on L_p and τ and cannot be directly measured.

By manipulating the foregoing relationships, the following expression for the apparent Lambertian reflectance of a surface target is found:

$$\rho = \frac{\pi(L_{sat} - L_p)}{H_{tot}\, e^{(-\tau \sec \theta_n)}} \qquad (6)$$

Solution of Equation 6 for a point of interest requires values of τ and L_p which are defined by conditions prevailing at the time of image acquisition. Ahern *et al.* (1977) proposed the use of oligotrophic lakes as standard reflectors which could be used to evaluate L_p by means of the expression

$$L_{sat} = (L_v + L_s + L_g)\,T + L_p \qquad (7)$$

where L_v is water volume radiance, L_s is water surface radiance, and L_g is sun glint radiance produced by solar zenith angles less than 30° or wave action due to strong winds. They defined $L_v = r_v H_{tot}$,

TABLE 3. MAXIMUM AND MINIMUM RADIANCE VALUES FOR LOW GAIN MODE OPERATION OF THE LANDSAT MULTISPECTRAL SCANNERS, TAKEN FROM ROBINOVE (1982) AND WARRINER (1983)

	Landsat 1		Landsat 2 6-22-75/7-16-75		Landsat 2 after 7-16-75		Landsat 3 3-5-78/6-1-78		Landsat 3 after 6-1-78		Landsat 4 9-16-82/4-1-83		Landsat 4 after 4-1-83	
Band	L_{min}	L_{max}	L_{min}	L_{max}	L_{min}	L_{max}	L_{min}	L_{max}	L_{min}	L_{max}	L_{min}	L_{max}	L_{min}	L_{max}
4	0	2.48	0.10	2.10	0.08	2.63	0.04	2.20	0.04	2.59	0.02	2.3	0.04	2.38
5	0	2.00	0.07	1.56	0.06	1.76	0.03	1.75	0.03	1.79	0.04	1.8	0.04	1.64
6	0	1.76	0.07	1.40	0.06	1.52	0.03	1.45	0.03	1.49	0.04	1.3	0.05	1.42
7	0	4.00	0.14	4.15	0.11	3.91	0.03	4.41	0.03	3.83	0.10	4.0	0.12	3.49

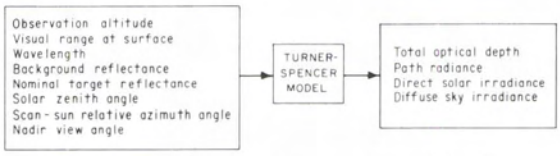

FIG. 2. Input and output parameters of the Turner-Spencer atmospheric radiative transfer model.

where r_v is water volume reflectance (sr^{-1}). Richardson *et al.* (1980) fitted equations to the field observations of Ahern *et al.* (1977) to obtain the equation

$$r_v = 0.0035 - 0.0036\,\lambda \qquad (8)$$

where λ is the wavelength of interest in the 0.4- to 3.0-μm range. They also used these observations to define $L_s = 0.006\,H_{sky}$. For the Canadian lake where Ahern *et al.* carried out their work, L_g was equal to zero. This was assumed to be the case for Flaming Gorge Reservoir as well. Solving of Equation 7 for L_p requires the use of the radiance over a clear lake appearing in the scene of interest and an appropriate atmospheric radiative transfer model.

Turner *et al.* (1971) and Turner and Spencer (1972) described a deterministic model of atmospheric radiative transfer which assumes a plane-parallel, homogeneous, aersol-filled atmosphere whose haze content is defined by the horizontal visual range at the surface. A schematic of the input and output parameters for the FORTRAN version of the model used in this study is presented in Figure 2. Specification of the visual range directly determines the value of total optical depth, τ, in the model which in turn permits calculation of path radiance, L_p. By specifying among the input parameters a visual range value that yields a path radiance value satisfying Equation 7 [i.e., $L_{sat} - (L_v + L_s + L_g)\,T - L_p \cong 0$)], one obtains results permitting the solution of Equation 6 for other scene targets in the vicinity. This visual range value must be found in an iterative fashion.

In applying the described method of accounting for atmospheric effects in Landsat imagery of Flaming Gorge Reservoir, it was assumed that uniform atmospheric conditions existed for the entire reservoir in any given scene of interest. Because air masses in the region are characteristically clear and dry and there are no adjacent urban areas which might introduce a nonhomogeneous distribution of aerosols, it was felt that this was a reasonable assumption. An area 20 pixels square in the main body of the reservoir near Lucerne Bay was selected as the oligotrophic standard reflector to provide radiances (L_{sat}) for the solution of Equation 7. Its location is indicated in Figure 1. This area was chosen because it is consistently characterized by extremely clear, deep waters free of bottom and edge effects. The latitude and longitude of this target were used in all calculations defining the scene geometry for

TABLE 4. LANDSAT SCENE DESCRIPTOR AND GEOMETRY DATA FOR OLIGOTROPHIC TARGET AT LATITUDE 40°58′, LONGITUDE 109°34′

Date	Landsat	Path-row	Altitude (km)	Z	θ_n	Relative Azimuth
22 September 1975	2	39–31	917	47.44	2.6	−142.2
17 September 1976	2	40–31	917	47.29	5.4	33.6
18 October 1977	2	40–31	917	58.51	2.3	38.7
2 August 1978	2	40–31	917	38.18	4.5	12.9
13 October 1978	2	40–31	917	55.80	4.5	39.9
9 September 1981	2	40–31	917	44.19	5.1	32.2
24 August 1982	4	37–31	705	38.85	3.1	28.3

use of the Turner-Spencer model. A solar ephemeris was used to compute solar zenith and azimuth angles for this target at the time of image acquisition. Scan azimuth and nadir view angles were approximated according to the location of the standard reflector target in the Landsat image. The relative azimuth angle required by the model was provided by subtracting the scan azimuth angle from the solar azimuth angle. Scene geometry data are presented in Table 4. Mean clear lake radiances appear in Table 5.

Application of the Turner-Spencer model also requires nominal target and background reflectance values as inputs. These were obtained by examining histograms for bands 4, 5, and 6 for a 2 August 1978 scene subset like that of Figure 1. The water and land modal digital counts were converted to radiance values by Equation 2 and used to solve the following approximation to Equation 6:

$$\bar{\rho} = \frac{\pi L_{sat}}{H_o \cos Z} \tag{9}$$

where $\bar{\rho}$ is the nominal reflectance in the band of interest, L_{sat} is the modal radiance for either land or water and H_o and Z are as defined before. The values obtained from the 2 August 1978 data were used in all runs of the model. They are presented in Table 6. Wavelength values of 0.55, 0.65, and 0.75 μm at the centers of bands 4, 5, and 6 were specified. Thus, for all seven scenes, the necessary input parameters for the model (refer to Figure 2) were determined, with the exception of visual range at the surface.

Three wavelengths were considered, then, for each of the seven reservoir scenes. For each case, the Turner-Spencer model was run iteratively with visual range specified as an integer value in kilometre units. The value specified was incremented in one-kilometre steps until that solution to Equation 7 with the smallest residual was found. Residual values were typically less than 0.001 mW/cm² sr. Model results obtained are presented in Table 7. With this accomplished, Equation 6 was used to calculate apparent Lambertian reflectance values for all surface sampling sites listed in Table 2. In this way, the remotely sensed observations were reduced to a form where they could be quantitatively related to the Secchi transparency and chlorophyll *a* observations of Table 1.

TABLE 5. MEAN RADIANCES (mW/cm² sr) FOR THE OLIGOTROPHIC STANDARD REFLECTOR FOR THE SEVEN SCENES ANALYZED

Date	Band 4	Band 5	Band 6
22 September 1975	0.2416	0.1280	0.0762
17 September 1976	0.2500	0.1335	0.0779
18 October 1977	0.2283	0.1138	0.0646
2 August 1978	0.2844	0.1493	0.0924
13 October 1978	0.2369	0.1366	0.0816
9 September 1981	0.2922	0.1596	0.0926
24 August 1982	0.2385	0.1408	0.0746

DEVELOPMENT OF WATER QUALITY IMAGES

Least-squares regression procedures were used to produce estimator equations for Secchi transparency and chlorophyll *a* concentration in terms of Landsat-derived reflectances. For Secchi transparency, the best equation found was

$$\frac{1}{SD} = 0.0665 + 35.6\rho_5 \tag{10}$$

where *SD* is Secchi transparency (metres) and ρ_5 is the apparent Lambertian reflectance for band 5. This equation was derived from data for 69 observations, with a coefficient of determination (r^2) of 0.94 and standard deviation about the mean of about 1.5 metres. The goodness of fit is illustrated in Figure 3. The best chlorophyll *a* predictor obtained was

TABLE 6. NOMINAL TARGET (WATER) AND BACKGROUND (LAND) REFLECTANCE ($\bar{\rho}$) USED WITH THE TURNER-SPENCER MODEL

Band	Water	Land
4	0.068	0.163
5	0.044	0.175
6	0.034	0.219

TABLE 7. RESULTS OBTAINED WITH THE TURNER-SPENCER MODEL FOR THE SEVEN LANDSAT SCENES OF FLAMING GORGE RESERVOIR

Date	Wavelength (μm)	Visual range (km)	L_p (mW/cm^2 sr)	τ	H_{tot} (mW/cm^2)
22 September 1975	0.55	44	0.2240	0.25612	8.469
	0.65	59	0.1138	0.15074	8.499
	0.75	61	0.0669	0.10788	7.356
17 September 1976	0.55	25	0.2316	0.33455	7.811
	0.65	42	0.1188	0.18700	8.199
	0.75	53	0.0682	0.12070	7.276
18 October 1977	0.55	19	0.2059	0.39126	5.531
	0.65	48	0.0963	0.17182	6.337
	0.75	61	0.0536	0.10788	5.637
2 August 1978	0.55	24	0.2712	0.34107	9.097
	0.65	42	0.1366	0.18700	9.563
	0.75	46	0.0834	0.13516	8.338
13 October 1978	0.55	18	0.2164	0.40445	5.908
	0.65	28	0.1172	0.24186	6.349
	0.75	38	0.0691	0.15744	5.766
9 September 1981	0.55	15	0.2762	0.45230	7.326
	0.65	26	0.1455	0.25350	8.100
	0.75	39	0.0827	0.15421	7.437
24 August 1982	0.55	68	0.2247	0.20707	10.371
	0.65	52	0.1284	0.16331	9.712
	0.75	76	0.0667	0.09051	8.655

$$\text{CHLA} = 1.37\, e^{(107\rho_6)} \qquad (11)$$

where CHLA is chlorophyll *a* concentration (mg/m^3) and ρ_6 is reflectance for band 6. Forty-four observations were used to develop this equation with $r^2 = 0.74$ and standard deviation about the mean of about 3.0 mg/m^3. Figure 4 illustrates its goodness of fit.

Development of Equations 10 and 11 made possible the production of color coded water quality images for all seven dates of interest. The objective of the study was to monitor year-to-year changes in the spatial distribution of general zones of trophic state. From an examination of historical records of Secchi transparency and chlorophyll *a* concentration, and the digital imagery, it was determined that the trophic intervals of Table 8 would yield meaningful maps of trophic spatial variability. For each scene of interest, then, color coding schemes were used to define two trophic state maps, one based on

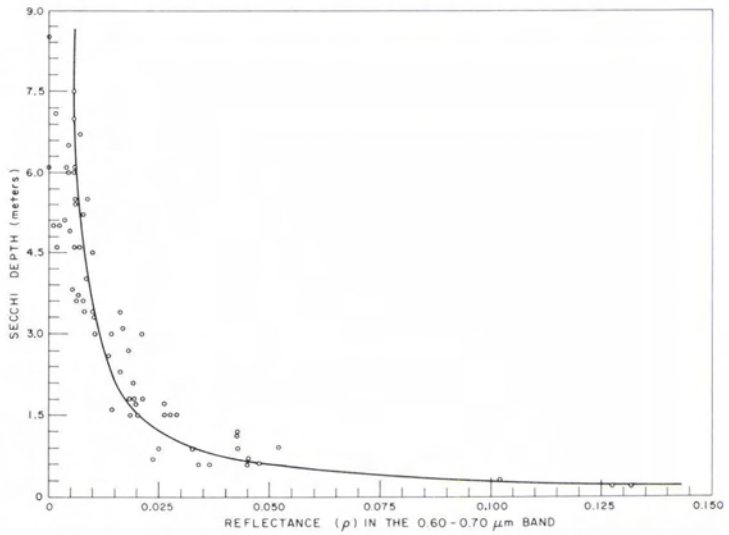

FIG. 3. Illustration of goodness of fit of Secchi transparency predictor equation.

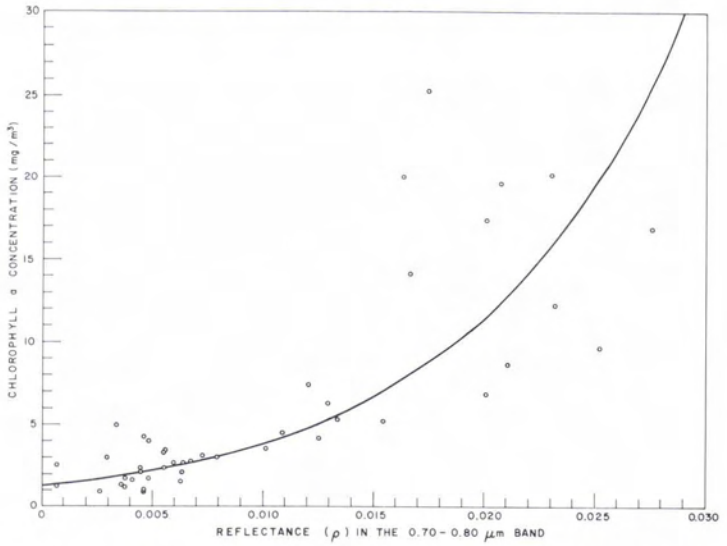

FIG. 4. Illustration of goodness of fit of chlorophyll *a* concentration predictor equation.

Secchi transparency and one based on chlorophyll *a* concentrations. Color photographic prints of these digital images were produced for limnological interpretation and analysis of the annual trends portrayed. Figures 5 and 6 present examples of the trophic zones identified with Equation 11.

One important consideration that arose was the potential confusion between turbidity due to suspended sediments and that due to the presence of algae. Areas of high suspended sediment concentration exhibit relatively high band 6 reflectances which, according to Equation 11, would suggest high concentrations of chlorophyll *a*. In reality, chlorophyll *a* concentrations are low in such areas due to the limitation of light available for photosynthesis. Fortunately, areas of organic and inorganic turbidity are normally spatially discrete in Flaming Gorge Reservoir, permitting the taking of steps to avoid this confusion. Meteorological records for the days immediately preceding image acquisition were examined to determine the likelihood of there being sediment plumes present. The relevant scenes were examined interactively in their digital form, and it was determined that those areas having Secchi transparencies less than 0.5 metre, according to Equation 10, had conditions of high suspended sediments. These areas were then masked out before applying Equation 11 and in this way erroneous es-

TABLE 8. INTERVALS OF SECCHI TRANSPARENCY AND CHLOROPHYLL *a* CONCENTRATION AND CORRESPONDING TROPHIC STATES

Trophic state	Secchi transparency (m)	Chlorophyll *a* concentration (mg/m^3)
Oligotrophic	>3	<4
Mesotrophic	1–3	4–10
Eutrophic	<1	>10

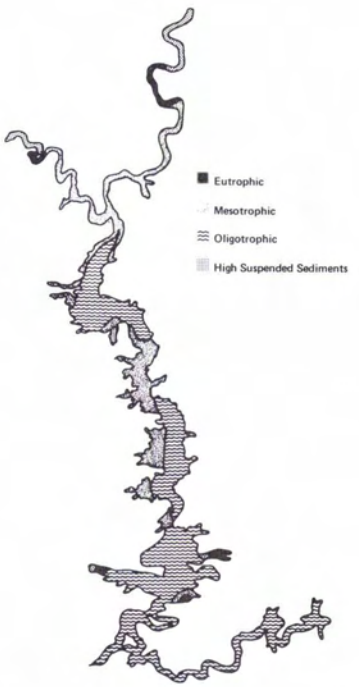

FIG. 5. Characterization of trophic states in Flaming Gorge Reservoir on 17 September 1976, as identified with Equation 11.

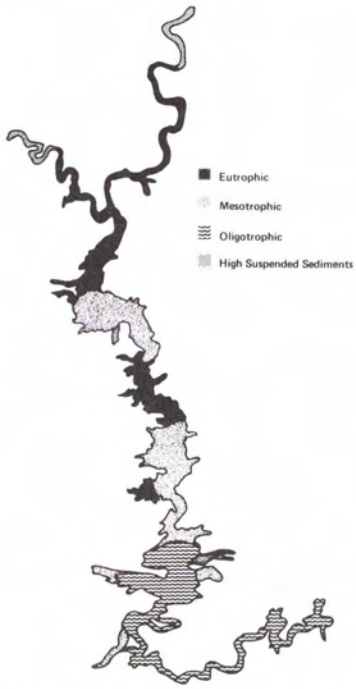

FIG. 6. Characterization of trophic states in Flaming Gorge Reservoir on 13 October 1978, as identified with Equation 11.

timates of trophic state, as defined by chlorophyll *a*, were avoided. Figures 5 and 6 show areas of high suspended sediments identified in this manner.

ASSESSMENT OF LANDSAT DATA CORRECTION TECHNIQUE

The method employed here for removal of atmospheric effects in the Landsat data necessarily involves simplifying assumptions to permit a practical modeling of complex physical processes. Ahern *et al.* (1977) back up their assumptions with an extensive set of field measurements and theoretical calculations. A full discussion of these issues, however, is beyond the scope of this paper. Nonetheless, the data on Flaming Gorge Reservoir may be used to assess the magnitude of the atmospheric effects that can be modeled with this approach.

Using the data from Table 1, a regression equation similar to Equation 10 was derived, with the difference that uncorrected band 5 digital counts were used instead of reflectance values. The equation yielded was

$$\frac{1}{SD} = -0.744 + 0.134\ DC_5 \qquad (12)$$

where DC_5 represents digital counts in band 5. The coefficient of determination (r^2) is 0.90 and the standard deviation about the mean 1.6 metres. The lower r^2 and higher standard deviation, when compared with the corresponding values for Equation 10, indicate a poorer goodness of fit when atmospheric correction has not been undertaken. Similarly, a chlorophyll concentration predictor equation was developed with digital count data: i.e.,

$$\text{CHLA} = 0.820\ e^{(0.354\ DC_6)} \qquad (13)$$

where DC_6 represents band 6 digital counts. Again, a poorer goodness of fit is seen when compared to the equation prepared from reflectance data, as evidenced by a lower coefficient of determination (0.68) and higher standard deviation about the mean (3.3 mg/m^3).

Although the coefficients of determination and standard deviations for Equations 12 and 13 are poorer than those for Equations 10 and 11, one might conclude that they are good enough for estimation purposes and that atmospheric correction of the satellite data could be dispensed with. What follows is an illustration of the potential pitfalls of such an assumption.

Consider, for example, a reservoir site with $\rho_5 = 0.025$. Using the scene geometry and atmospheric properties for 18 October 1977, from Tables 4 and 7, one may in turn compute a corresponding digital count by means of Equations 1 and 2. This value, $DC_5 = 5.9$, when substituted into Equation 12, yields an estimate of Secchi transparency of 21.4 metres, which would suggest an ultra-oligotriphic condition. By contrast, if scene geometry and atmospheric properties for 2 August 1978 are used, a value of $DC_5 = 10.4$ is obtained. Substitution of this value into Equation 12 gives an estimated Secchi transparency of 1.5 metres, a mesotrophic condition.

Similarly, a reservoir site with $\rho_6 = 0.015$ would exhibit a digital count of 1.5 under the conditions of 18 October 1977 as compared with a digital count of 5.1 for 2 August 1978. When these values are substituted into Equation 13, chlorophyll concentration estimates of 1.4 mg/m^3 and 5.0 mg/m^3, respectively, are obtained. In the first case, oligotrophic conditions are indicated, whereas in the second case, the chlorophyll concentration estimate suggests a mesotrophic state. Quite clearly, an accounting for atmospheric effects is required if multidate satellite data are to be used to reliably estimate reservoir trophic state.

LOCATIONAL ERRORS

One troublesome aspect of the data anlaysis procedures was the difficulty in reliably identifying surface sample sites in the Landsat scenes. It is believed that this problem contributes to the significant difference in goodness of fit between Equations 10 and 11. The spatial variation of Secchi transparency, a characteristic of the water column as a whole, is usually not sharply defined and seems to agree fairly well with remote sensing measurements regardless of errors in sample site location. Chlorophyll *a* concentration, on the other hand, can vary

markedly within short distances, because algae blooms are very patchy. Regression on Landsat data is therefore more sensitive to these locational errors. The observed decrease in goodness of fit for Equation 11 with increasing chlorophyll concentration is consistent with such a situation. A possible remedy might be the carrying of a Loran-C navigation unit by field sampling crews. Landsat imagery could be mathematically linked to a map grid prior to analysis, and sample sites located subject only to the quantifiable inaccuracies of the coordinate transformation and the navigation system.

Summary and Conclusions

Using data collected on Flaming Gorge Reservoir, it has been shown that an accounting for atmospheric effects in Landsat imagery permits the development of a single set of water quality predictive equations from measurements obtained on several different dates. Such an approach also permits estimation of reservoir trophic state from image data acquired on dates for which there is no concurrently acquired surface sampling data. Failure to account for atmospheric effects when working with multidate imagery can potentially lead to erroneous assessments of reservoir trophic state. This was illustrated with hypothetical examples. The potential for errors in the approach due to uncertainty in locating sample sites in the image data was noted, along with the possible effects on regression goodness of fit this might cause. In spite of these problems, it is felt that the work described here represents a successful application of satellite remote sensing to the monitoring of water quality in a large Bureau of Reclamation reservoir. Given the costs of conducting surface sampling of such a reservoir, the results suggest that sampling designs should routinely incorporate remote sensing techniques in order to magnify the benefits of these measurements by extrapolating them spatially and temporally. The contribution to understanding reservoir limnology appears to be significant.

Acknowledgments

Richard Blackwell, of the Jet Propulsion Laboratory, and Dennis Nelson, of the Environmental Protection Agency, provided the 2 August 1978 Flaming Gorge Data. Arthur J. Richardson, of the U.S. Department of Agriculture-Agricultural Research Service, made available a copy of the FORTRAN code of the Turner-Spencer model.

References

Ahern, F., D. Goodenough, S. Jain, V. Rao, and G. Rochon, 1977. Use of Clear Lakes as Standard Reflectors for Atmospheric Measurements, *Proceedings of the Eleventh International Symposium on Remote Sensing of the Environment*, Environmental Research Institute of Michigan, Volume 1, pp. 731-755.

Grimshaw, H., C. Barb, J. Harrington, S. Torrano, and H. Brown, 1980. *Classification of Oklahoma Reservoirs Using Landsat Multispectral Scanner Data*, Oklahoma Water Resources Board Publication 104, Oklahoma City, 153 p.

Hoffer, R., 1978. Biological and Physical Considerations in Applying Computer-Aided Analysis Techniques to Remote Sensor Data, Chapter 5 in *Remote Sensing: The Quantitative Approach*, P. Swain and S. Davis, Editors, McGraw-Hill, 396 p.

Lillesand, T., W. Johnson, R. Deuell, O. Lindstrom, and D. Meisner, 1983. Use of Landsat Data to Predict the Trophic State of Minnesota Lakes, *Photogrammetric Engineering and Remote Sensing*, Volume 49, No. 2, pp. 219-229.

Martin, R. H., E. O. Boebel, R. C. Dunst, O. D. Williams, M. V. Olsen, R. W. Meredith, and F. L. Scarpace, 1983. *Wisconsin's Lakes: A Trophic Assessment Using Landsat Digital Data*, Inland Lake Renewal Section, Wisconsin Department of Natural Resources, Madison, Wisconsin, 294 p.

Meinert, D., D. Malone, A. Voss, and F. Scarpace, 1980. *Trophic Classification of Tennessee Valley Area Reservoirs Derived from Landsat Multispectral Scanner Data*, Tennessee Valley Authority, 66 p.

Olsen, M., R. Meredith, F. Scarpace and R. Martin, 1981. Recent Investigations with a Satellite Lake Trophic Classification Program (abstract), in *Proceedings of the American Society of Photogrammetry Fall Technical Meeting*, San Francisco, 629 p.

Richardson, A., D. Escobar, H. Gausman, and J. Everitt, 1980. Comparison of Landsat 2 and Field Spectrometer Reflectance Signatures of South Texas Rangeland Plant Communities, *Proceedings of the 1980 Machine Processing of Remotely Sensed Data Symposium*, Purdue University, pp. 88-97.

Robinove, C., 1982. Computation with Physical Values from Landsat Digital Data, *Photogrammetric Engineering and Remote Sensing*, Volume 48, No. 5, pp. 781-784.

Rogers, R., and K. Peacock, 1973. Machine Processing of ERTS and Ground Truth Data, *Machine Processing of Remotely Sensed Data*, IEEE Catalog No. 73, CHO 834-2GE, p. 4A: 14-27.

Thekaekara, M., R. Kruger, and C. Duncan, 1969. Solar Irradiance Measurements from a Research Aircraft, *Applied Optics* 13(3): 518-522.

Turner, R., W. Malila, and R. Nalepka, 1971. Importance of Atmospheric Scattering in Remote Sensing, *Proceedings of the Seventh International Symposium on Remote Sensing of the Environment*, Environmental Research Institute of Michigan, volume 3, pp. 1651-1697.

Turner, R., and M. Spencer, 1972. Atmospheric Model for Correction of Spacecraft Data, *Proceedings of the Eighth International Symposium on Remote Sensing of Environment*, Environmental Research Institute of Michigan, pp. 895-934.

Verdin, J., 1983. Corrected vs. Uncorrected Landsat 4 MSS Data, *Landsat Data Users Notes*, June 1983, National Oceanic and Atmospheric Administration, pp. 4-8.

Verdin J., and D. Wegner, 1983. Development of Reservoir Water Quality Gradients from Multispectral

Scanner Imagery, *Proceedings of the 1983 Fall Meeting of the American Society of Photogrammetry*, Salt Lake City, pp. 585-594.

Warriner, H., 1983. *Public release of the Landsat Production Program Manager*, National Oceanic and Atmospheric Administration, EROS Data Center, Sioux Falls, South Dakota, March 30, 1 p.

Wegner, D., 1982. Limnological Environment of Flaming Gorge Reservoir, *Proceedings of the 1982 Western Division Meeting of the American Fisheries Society*, Las Vegas, 12 p.

Witzig, A., and C. Whitehurst, 1981. Literature Review of the Current Use and Technology of MSS Digital Data for Lake Trophic Classification, *Proceedings of the 1981 Fall Meeting of the American Society of Photogrammetry*, San Francisco, pp. 1-20.

(Received 29 August 1983; revised and accepted 17 November 1984)

International Space Policy: Options for the Twentieth Century and Beyond

Atlanta, Georgia
16-17 May 1985

This two-day conference—sponsored by the Georgia Institute of Technology's Program in Science, Technology, and International Affairs—will focus on the generic issues of international space policy and, more specifically, the range of issues and options in the areas of

- U.S. policy towards international space issues
- The political and diplomatic dimension of international space policy
- The military/strategic dimension of international space policy
- The commercial/competitive dimension of international space policy

For further information please contact

Dr. John R. McIntyre
School of Social Sciences
The Georgia Institute of Technology
Atlanta, GA 30332
Tele. (404) 894-3195

Forthcoming Articles

James E. Anderson, The Use of Landsat-4 MSS Digital Data in Temporal Data Sets and the Evaluation of Scene-to-Scene Registration Accuracy.

O. O. Ayeni, Photogrammetry as a Tool for National Development.

Arthur J. Brandenberger and *Sanjib K. Ghosh*, The World's Topographic and Cadastral Mapping Operation.

J. H. Everitt, *A. J. Richardson*, and *H. W. Gausman*, Leaf Reflectance-Nitrogen-Chlorophyll Relations in Buffelgrass.

B. C. Forster, Principle and Rotated Component Analysis of Urban Surface Reflectances.

Armin W. Gruen, Algorithmic Aspects in On-Line Triangulation.

Ellsworth F. LeDrew and *Steven E. Franklin*, The Use of Thermal Infrared Imagery in Surface Current Analysis of a Small Lake.

Ross Nelson, Reducing Landsat MSS Scene Variability.

Laurence L. Strong, *Robert W. Dana*, and *Len H. Carpenter*, Estimating Phytomass of Sagebrush Habitat Types from Microdensitometer Data.